Eur. Phys. J. D **24**, 393–396 (2003)
DOI: 10.1140/epjd/e2003-00174-9

THE EUROPEAN PHYSICAL JOURNAL D

Dynamical aspects of thermionic emission of C_{60} studied by 3D imaging

F. Lépine[1], B. Climen[1], F. Pagliarulo[1], B. Baguenard[1], M.A. Lebeault[1], C. Bordas[1,a], and M. Hedén[2]

[1] Laboratoire de Spectrométrie Ionique et Moléculaire[b], CNRS and Université Lyon 1, bâtiment A. Kastler, 43 boulevard du 11 novembre 1918, 69622 Villeurbanne Cedex, France
[2] School of Physics and Engineering Physics, Göteborg University and Chalmers University of Technology, 41296 Göteborg, Sweden

Received 10 September 2002
Published online 3 July 2003 –

Abstract. We present the first experimental results of the time-dependent photoelectron spectrum observed in thermionic emission of hot C_{60} excited by multiphoton absorption. Time resolved velocity-map imaging is used to record photoelectron spectra. As opposed to the evolution of the total photoelectron current that follows a power law as a function of the delay after excitation, it is shown that the photoelectron spectrum bears precise information on the degree of excitation of the ensemble of clusters. The effective temperature deduced from the experimental spectrum is found to be directly related to the average internal energy in the initial step of the decay, while after typically 1 μs the photoelectron spectrum is almost independent on the initial excitation process. The subsequent evolution of the spectrum as a function of the time-delay after excitation is found to be very slow.

PACS. 36.40.-c Atomic and molecular clusters – 33.60.Cv Ultraviolet and vacuum ultraviolet photoelectron spectra

1 Introduction

Excited clusters offer many experimental situations to study thermodynamics in finite-size systems. Among these, the study of thermionic emission is particularly interesting for refractory systems. However, many experimental results available in the literature are not consistent and large discrepancies have been reported for similar systems excited under comparable conditions depending on the experimental method used and on the observation time-window. Therefore, only a complete approach, combining the measurement of the kinetic energy distribution of all fragments with the determination of the time-evolution of the total electron (or fragment) emission rate may reconcile the various observations. This statement has motivated our study of time-dependent thermionic emission photoelectron spectra in neutral C_{60} where the large timescales involved allow the combination of measurements both in the energy and in the time domain.

Delayed ionization from C_{60} has been a subject of great interest in the past few years [1–7] however the clarification of the most important features has not been achieved until the analysis carried out by Hansen and Echt [8]. Indeed, many groups have tried to analyze the time dependence of the electron emission in term of rate constants. In most cases, experimental data could be fitted only using multiexponential decay curve with rate constants ranging from 10^4 to 10^7 s^{-1} under comparable experimental situations irrespective of the laser wavelength (above typically 200 nm) or fluence (at least in the nanosecond regime). The main differences arise in fact from the time-window used for the fitting procedure. Indeed, owing to the multiphoton excitation of C_{60} required for photoionization, the internal energy of the excited clusters does not take a single value such as in the microcanonical ensemble case. On the contrary, the internal energy may be represented by a broad distribution and the concept of a microcanonical ensemble of clusters all with the same internal energy that can be described by a single microcanonical temperature and a single emission rate is totally irrelevant and must be revised accordingly to the excitation process. As known for example from nuclear physics, the emission current of an ensemble of systems with a broad internal energy distribution, with individual rates k depending on the internal energy, is the sum of individual exponential profiles $\exp(-kt)$ that result in a $1/t$ law provided the energy distribution is broad enough. In addition, as demonstrated in [8], if the electron emission process is in competition with another decay channel (emission of C_2 fragments), this simple power law is

[a] e-mail: bordas@lasim.univ-lyon1.fr
[b] UMR 5579

modified and must be replaced by a more general power law t^{-p}, with the parameter p being directly connected to the ratio of the corresponding emission barrier of both competing processes. After longer delay, typically above 10 μs, the emission current deviates from this simple power law. The competition with other processes such as blackbody radiation or delayed ionization from electronically excited fullerenes in the lowest triplet states has been invoked to explain this departure [9,10]. In the following, we focus on the electron emission of fullerenes at relatively short times in the range 0–10 μs where the major part of the emission occurs and we will neglect for the moment competition with other decay channels.

A total emission rate governed by a power law as a function of time is characteristic of an ensemble of small free particles with a broad internal energy distribution undergoing thermally activated decay. Since this emission law has a profile completely independent of the degree of excitation of the emitting systems, the information drawn from its measurement is rather limited. In particular there is no signature in the observed decay of the average internal excitation of the clusters. In other words the observed decay has nothing to do with the effective temperature of the ensemble and no connection between emission rate and effective temperature can be drawn from such measurement. On the other hand, it maybe suspected that the energy spectrum of the emitted electrons should bear some information about this temperature. In addition, since highly excited clusters decay more rapidly than those having a lower excitation, the average energy, or temperature, is expected to decrease as a function of the time delay after excitation. In that sense, we expect the information contained in the time-dependent energy spectrum to be a precise measurement of the average degree of excitation of the systems, allowing to follow the evolution of the dynamics of the hot fullerenes.

2 Simple model of thermionic emission

So far, only the time dependence of thermal electron emission in C_{60} has been addressed. In this paper we report on the first experimental results in photoelectron imaging spectroscopy allowing the measurement of the electron energy distribution as a function of the time delay with respect to excitation. As for the emission current but in the energy domain, the total emission spectrum results from the summation of a continuum of microcanonical contributions depending on the internal energy E. In the case of thermionic emission from a neutral species, every individual microcanonical kinetic energy distribution is represented by a decreasing exponential term as a function of the electron kinetic energy. In addition, the internal energy distribution evolves with time as the clusters undergo thermal decay. Let us now describe briefly the general features of our simple model describing the thermionic emission spectra of hot C_{60}. Following the general formulation of statistical emission processes [11] and its application to thermal decay processes in clusters [12–15] we introduce the differential thermionic emission rate $k_e(E,\epsilon)$ that may be written as

$$k_e(E,\epsilon) = \frac{2m}{\pi^2\hbar^3}\sigma(\epsilon)\epsilon \exp\left(\frac{-\epsilon}{k_b T_d}\right)\exp\left(\frac{-\Phi}{k_b T_e}\right) \quad (1)$$

where E is the internal energy of the cluster, ϵ is the kinetic energy of the ejected electron, $\sigma(\epsilon)$ is the cross-section for electron capture, T_d and T_e are respectively the daughter temperature and the emission temperature and Φ the ionization potential. We assume the following relation [14] between the energy E and the microcanonical temperature (C_v is the microcanonical heat capacity from [21]).

$$T_d = \frac{E-\Phi}{C_v} \quad \text{and} \quad T_e = \frac{E-\Phi/2}{C_v}\cdot \quad (2)$$

The cross-section appearing in equation (1) is the Coulombic capture cross-section (R_0 is the radius of C_{60} (3.5 Å))

$$\sigma(\epsilon) = \frac{\pi e^2}{4\pi\epsilon_0}\frac{R_0}{\epsilon}\cdot \quad (3)$$

The microcanonical thermionic emission rate $k_e(E)$ is then given by

$$k_e(E) = \int_0^\infty k_e(E,\epsilon)\mathrm{d}\epsilon = \frac{2m}{\pi^2\hbar^3}\frac{e^2R_0}{4\pi\epsilon_0}k_B T_d \exp\left(\frac{-\Phi}{k_B T_e}\right)\cdot \quad (4)$$

At this stage, the competition with other decay channels is neglected. The time-dependent electron spectrum is then found by integrating over all possible internal energies. Assuming an initial energy distribution (Poisson-like in the following) after laser excitation $g(E)$, The time-dependent electron spectrum is expressed as:

$$P(\epsilon,t) = \int_0^\infty k_e(E,\epsilon)g(E)\exp\left(-tk_e(E)\right)\mathrm{d}E. \quad (5)$$

Provided that the energy distribution $g(E)$ is broad enough, which is always the case in multiphoton excitation above ionization threshold of C_{60} with visible or UV light, the total electron current is proportional to t^{-1}. Note that the correct behavior t^{-p}, with $p \approx 0.64$ [8] would be found by inserting the fragmentation channel. However, since at this point we merely need to find the qualitative behavior of the electron spectrum, we neglect this contribution.

Without going into the details of the simulations that will be exposed elsewhere, the major results of this simple model may be summarized as follows.

1. The evolution of the microcanonical thermionic emission rate $k_e(E)$ as given by equation (4) is extremely rapid with the energy as visible in Figure 1. As a consequence, the contribution to the thermionic emission current at a given delay time is dominated by the rather narrow energy-range having an emission rate inversely proportional to that time-delay.
2. It follows that the time-dependent photoelectron spectrum (Eq. (6)) resulting from the summation of a continuum of exponential terms (Eq. (1)) remains very close to a simple exponential (microcanonical) term.

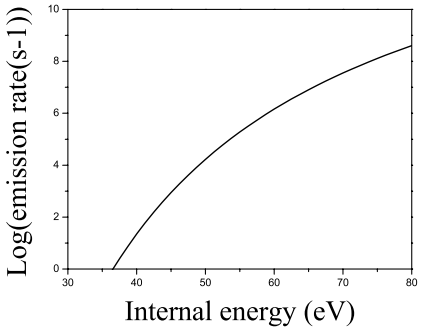

Fig. 1. Logarithm of the electron emission rate as a function of the internal energy.

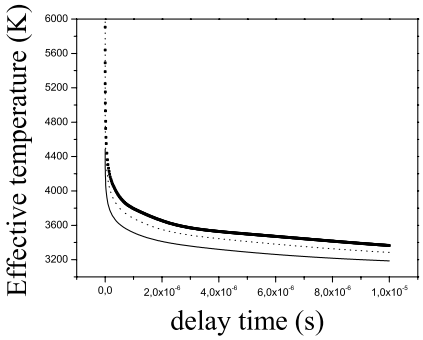

Fig. 2. Time-evolution of the effective temperature. $N = 5$ photons (solid line), $N = 10$ photons (dotted-line), $N = 20$ photons (broad solid-line) ($\lambda = 330$ nm).

The combination of these two findings results in:

– an effective temperature varying with the time-delay may be associated with the resulting total energy distribution. At short time delay this temperature is linked to the energy of the most excited fullerenes. After a finite delay-time τ, and owing to remark (1), the effective temperature T^* is mainly determined by a given class of clusters with the appropriate emission rate $k_e(E^*) \approx 1/\tau$ with the microcanonical temperature T^* being the daughter temperature $T_d(E^*)$ as given by equation (2). This can be written:

$$P(\epsilon, t) \approx \exp\left(\frac{-\epsilon}{k_b T^*}\right) \int_0^\infty A(E) g(E) \exp(-t k_e(E)) \mathrm{d}E \tag{6}$$

$A(E)$ is linked to the rate constant;

– the photoelectron spectrum evolves very smoothly as a function of the time delay after optical excitation. Only the initial degree of internal excitation, which depends on the fluence of the exciting laser beam, significantly affects the energy profile in the initial stage of the emission process. Afterwards, the time-dependent emission spectrum is roughly independent on the initial average excitation energy and narrows slowly with time-delay.

The time evolution of the effective temperature is presented in Figure 2 in the case of an initial excitation corresponding to a Poisson distribution centered around $N = 5$, $N = 10$ and $N = 20$ photons at $\lambda = 330$ nm. In the case of $N = 10$ photons the effective temperatures expected are 5300 K ($t = 0$ μs), 3700 K ($t = 1$ μs) and 3300 K ($t = 10$ μs). Note that the very high temperature at short delays corresponds to the hot wing of the energy distribution. The corresponding energy spectrum is indeed very close to a microcanonical distribution. This is simply due to the fact that the contribution at a given time-delay is completely dominated by a very narrow energy range as noted above and as visible from Figure 1.

3 Experiment

In order to measure photoelectron spectra as a function of the time-delay after optical excitation, we have built a new velocity-map [16] 3D-imaging set-up combining the position-sensitive-detection capabilities of the velocity-map imaging with electronic gating of the detector. The principle of photoelectron imaging spectroscopy is briefly as follows. Photoelectrons arising from an ionization process are accelerated by a uniform electric field onto a position-sensitive-detector (PSD) consisting of a pair of microchannel plates followed by a phosphor screen read *via* a digital CCD camera. The accumulation of electron impacts on the detector results in an image that contains the distribution of the projection of the initial velocity of the electrons onto the plane of detection. By choosing the laser polarization parallel to the detector, a simple inversion method [17] allows to derive the initial velocity distribution and therefore the energy spectrum. In velocity-map imaging, an inhomogeneous electric field is used in order to get an impact position on the PSD depending only on the initial velocity irrespective of the initial position in the interaction region. As opposed to traditional photoelectron spectrometer such as magnetic-bottle, the gating of the PSD allows the study of the evolution of the kinetic energy distribution of photoelectrons as a function of the time-delay after optical excitation, with a time resolution of the order of 100 ns. Since it is based on a purely geometrical measurement of the initial velocity, velocity map imaging allows obtaining kinetic energy spectra for different time-windows after excitation. In addition, the detection efficiency of velocity-map imaging does not depend on the initial kinetic energy. This is specifically interesting at threshold since it allows measuring slow photoelectron energy distribution, particularly relevant for the study of thermal electron emission from hot clusters [18–20]. The beam of cold C_{60} is produced by laser desorption of pure C_{60} embedded in a rod of organic material (matrix-assisted laser desorption). The optical excitation of the fullerenes is achieved in the interaction region of the velocity-map imaging spectrometer. Various experiments have been carried out in the range 220 to 400 nm, at laser fluences below 10^{-9} W/cm^2. Optical excitation is performed using an amplified OPO laser (pulse duration 8 ns, 5 to 50 mJ per pulse).

Figure 3 presents a typical photoelectron spectrum recorded at $\lambda = 330$ nm under the same experimental

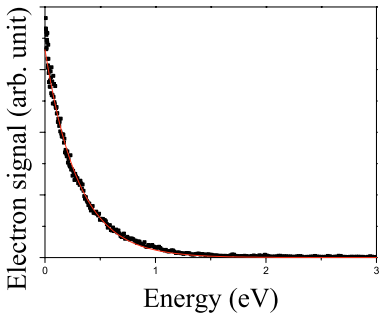

Fig. 3. Experimental spectrum (dots) at 1 μs fitted (solid line) with $T = 3500$ K.

conditions. This spectrum results from the inversion of an electron image recorded at a time-delay of 1 μs after optical excitation. Note that for a null delay (*i.e.* detection of prompt electrons) thermal electrons arising from thermionic emission from C_{60} are detected together with prompt electrons arising from the photofragmentation processes giving rise to lighter (prompt) ions. Therefore the $t = 0$ spectrum is not a pure thermionic emission spectrum and it is not relevant for estimating the initial degree of internal excitation.

As predicted in the preceding section, the evolution of the photoelectron spectrum with time delay is found to be rather slow. Spectra recorded at shorter delay (larger than 100 ns) are not significantly different within our experimental resolution, while at longer delay a weak decrease of the effective temperature is observed. A least-square fitting of the spectrum of Figure 3 leads to and effective temperature $T \approx 3500$ K , in excellent agreement with our simple model predicting $T \approx 3700$ K after a 1 μs delay. Including dissociation in our simulation decreases in fact this temperature by a significant amount and improves the agreement with experimental results. Also in good agreement with our predictions, varying the laser fluence does not influence significantly this effective temperature after a finite delay time. Indeed, although multiphoton ionization is a strongly non-linear process, the limitation inherent to the use of a nanosecond laser prevents the exploration of a broad range of effective temperature. In addition and as noted above, the effective temperature deduced from the spectrum is in fact directly connected to the time-delay at which the spectrum is recorded *via* the microcanonical emission rate. Despite these limitations in the range of our observations, the present experimental results confirm without ambiguity the validity of our approach and show that supplementary information may be drawn from measurement of time-dependent photoelectron spectra.

4 Conclusion

The present experimental results are the first measurements allowing to follow the evolution of the photoelectron kinetic energy spectrum as a function of the time-delay after multiphoton ionization of C_{60}. In the range of laser fluences and time domain explored here, our observations strongly support the statistical character of the C_{60} decay *via* emission of electrons, justifying its denomination as thermionic emission. Our simple model together with our experimental results show that the effective temperature T^* of a photoelectron spectrum recorded after a given delay τ corresponds approximately to systems having a microcanonical emission rate $k_e(E^*) \approx 1/\tau$ with $T^* = T_d(E^*)$. Therefore, time-dependent photoelectron spectroscopy allows the direct experimental determination of the total decay rate as a function of the microcanonical temperature. Our simple approach is presently being improved by including explicitly the dissociation decay channels in equation (6).

We acknowledge the support of the European Network Cluster Cooling, contract No. HPRN-CT-2000-00026.

References

1. C.E. Klots, Z. Phys. D **20**, 105 (1991)
2. E.E.B. Campbell, G. Ulmer, I.V. Hertel, Phys. Rev. Lett. **67**, 1986 (1991)
3. P. Sandler, C. Lifshitz, C.E. Klots, Chem. Phys. Lett. **200**, 445 (1992)
4. Y. Zhang, M. Stuke, Phys. Rev. Lett. **70**, 3231 (1996)
5. D. Ding, J. Huang, R.N. Compton, C.E. Klots, R.E. Haufler, Phys. Rev. Lett. **73**, 1084 (1994)
6. C.E. Klots, R.N. Compton, Surf. Sci. Lett. **3**, 535 (1996)
7. E.E.B. Campbell, R.D. Levine, Annu. Rev. Phys. Chem. **51**, 65 (2000)
8. K. Hansen, O. Echt, Phys. Rev. Lett. **12**, 2337 (1997)
9. F. Rohmund, M. Hedén, A.V. Bulgakov, E.E.B. Campbell, J. Chem. Phys. **115**, 3068 (2001)
10. J.U. Andersen, C. Gottrup, K. Hansen, P. Hvelplund, M.O. Larsson, Eur. Phys. J. D **17**, 189 (2001)
11. V. Weisskopf, Phys. Rev. **52**, 295 (1937)
12. C.E. Klots, J. Chem. Phys. **100**, 1035 (1994)
13. K. Hansen, Phil. Mag. B **79**, 1413 (1999)
14. J.U. Andersen, E. Bonderup, K. Hansen, J. Chem. Phys. **114**, 6518 (2001)
15. J.U. Andersen, E. Bonderup, K. Hansen, J. Phys. B **35**, R1 (2002)
16. A.T.J.B. Eppink, D.H. Parker, Rev. Sci. Instr. **68**, 3477 (1997)
17. C. Bordas, F. Paulig, H. Helm, D.L. Huestis, Rev. Sci. Instr. **67**, 2257 (1996)
18. J.C. Pinaré, B. Baguenard, C. Bordas, M. Broyer, Phys. Rev. Lett. **81**, 2225 (1998)
19. B. Baguenard, J.C. Pinaré, C. Bordas, M. Broyer, Phys. Rev. A **63**, 023204 (2001)
20. B. Baguenard, J.C. Pinaré, F. Lépine, C. Bordas, M. Broyer, Chem. Phys. Lett. **352**, 147 (2002)
21. B. Tsipinyuk, A. Budrevich, M. Grinberg, E. Kolodney, J. Chem. Phys. **106**, 2449 (1997)